A. K. Gupta
K. Singh
Indian Institute of Technology
New Delhi-110029, India

Bar Spread Functions for Parabolic Image Motion

The effect of parabolic image motion in panoramic cameras becomes significant for large obstruction ratios.

Introduction

SINGLE BAR ANALYSIS recently has acquired importance in the assessment of optical systems and is of direct importance in aerial photography[1] because the projected silhouettes of the objects such as pipes, rails, white road lines, highways, etc., are effectively single bar objects and their imagery is of considerable importance. For an infinitesimally thin bar, one obtains the line spread function. On the other hand, with a very

thus, various aspects of the images formed by annular apertures need extensive investigation. An extensive list of relevant references is given elsewhere[7,8]. Some recent relevant studies may also be noted[9–15].

Most of the investigations have dealt with diffraction/aberration limited systems. However, greater and greater precision is being demanded of motion sensing and image motion compensation (IMC) equipment as precision in aerial reconnaissance,

ABSTRACT: *A graphical analysis has been made of the image intensity distribution for bar targets of varying widths in presence of parabolic image motion for various sizes of the pupil-obscuration in panoramic cameras. Asymmetry in the intensity distribution in the image has been investigated in detail. For large obstruction ratios, deleterious effects of motion become very significant and the tolerance on the image motion appears to become very stringent. Results also have been obtained for the image of two other isolated extended objects, namely a triangle and an object in the shape of a single cycle of pure sinusoid. The line spread function has also been obtained and single bar contrast functions plotted.*

wide bar the image may be similar to that of an edge. A bar image can also be synthesized as the difference of the two edge spread functions[1]. A single bar also has found application as a resolving power test target[1-3] and the methods of defining and calculating the contrast of bar images have been developed[4-6]. Generally, the imaging system is considered to have a circular aperture.

Annular aperture systems are also of considerable importance and more interesting than the conventional circular aperture systems. The central portion of the Airy pattern in such a system becomes narrower and thus increases the depth of focus of the system;

surveillance and other intelligence activities increases. Since IMC techniques are never perfect, some residual image motion[16–20] is always present and for a significant class of problems puts a limit to the resolution. Vibrations from machinery close by, the spinning or tumbling of the spacecraft, the jerking of the camera by the hand of an astronaut and even the click of the camera shutter are some typical sources of image motion[16 through 20]. Effects of linear and sinusoidal motion on the images of various objects have been extensively investigated[21–23] in the past.

Interest in transverse scanning panoramic aerial cameras[17–24] has stimulated con-

siderable analysis of their performance characteristics. Two forms of transverse scanning panoramic cameras are available. The first has film fixed upon a cylindrical focal surface and sweeps the image across the film by swinging the lens itself; the second has a fixed lens and slit arrangement accomplishing the transverse scan by rotating a mirror or a prism in front of the lens and synchronising this with the motion of the film past the slit. The image motion in these is compensated by moving the optics or the film in some way that will minimize the over-all image motion.

Residual image motion in transverse scanning panoramic cameras results from the finite slit width which precludes the film's IMC from being exactly correct for all images simultaneously exposed in the slit. The image displacement is a parabolic function of time[17-26]. Such motion recently has been considered with respect to its effect on imagery[26] holographic measurements[27] and image restoration[28,29].

We have discussed the single bar targets in the presence of parabolic image motion for annular aperture systems. The results for a triangle and an object having the shape of a single cycle of pure sinusoid are also included.

THEORY

The image intensity spectrum $I(\omega)$ and the object intensity spectrum $O(\omega)$ are related by

$$I(\omega) = T(\omega) O(\omega) \qquad (1)$$

where $T(\omega)$ is the optical transfer function of the system and ω the normalised spatial frequency. Intensity distribution $i(V)$ in the image is the inverse Fourier transform of $I(\omega)$. Hence

$$i(V) = \int_{-\infty}^{\infty} T(\omega) O(\omega) \exp (iV\omega)d\omega \qquad (2)$$

where V is the distance in the image plane in diffraction units*. Since a one-dimensional Fourier transform has been written in Equation 2, the formula is applicable only to images of one-dimensional objects. The object spectrum $O(\omega)$ can be obtained by taking the Fourier transform of the object intensity function $O(V)$. For a single bar[22,30] this turns out to be

$$O(\omega) = (\pi\omega)^{-1} \sin (\omega L) \qquad (3)$$

* $V = \pi x/\lambda F$ where x is linear distance in the image plane from optical axis, λ is wavelength of radiations, and F is the f-number of the optical system under consideration.

where $2L$ is the width of the bar in diffraction units. Since $T = T_r - iT_i$ where T_r and T_i are respectively the even and odd function of ω, $i(V)$ reduces to

$$i(V) = 2(\pi)^{-1} \left[\int_0^2 T_r(\omega) \sin (\omega L) \cos (V\omega) \right.$$
$$(\omega^{-1})d\omega + \int_0^2 T_i(\omega) \sin (\omega L) \sin \qquad (4)$$
$$(V\omega) (\omega^{-1}) d\omega$$

Since $T(\omega)$ vanishes for $\omega > 2$, the limits of the integral have been taken from 0 to 2. The optical transfer function of a diffraction limited system may now be multiplied by the optical transfer function of the motion to give the transfer function of a system afflicted with motion-induced image degradation. Hence

$$T(\omega) = D(\omega) C(\omega) \qquad (5)$$

where $D(\omega)$ is the diffraction limited MTF and $C(\omega)$, the motion OTF.

The expression for $D(\omega)$ in case of an annular aperture is well known[7,8].

Further, the OTF for parabolic motion[17,24,25] is given by

$$C(\omega) = \frac{\sqrt{I_1^2 + I_2^2}}{2\sqrt{\omega A}} e^{-i \theta'} \qquad (6)$$

Here $\theta' = \tan^{-1} (I_2/I_1)$ is the phase lag and I_1 and I_2 are the Fresnel's integrals given by

$$I_1 = \int_0^{2\sqrt{\omega A}} \cos (\pi/2 \, u^2)du \qquad (7)$$

$$I_2 = \int_0^{2\sqrt{\omega A}} \sin (\pi/2u^2) \, du$$

A is the dimensionless motion parameter given by $A = Bte^2/2\lambda F$. Here B is defined by the equation of the parabolic motion[17], te is total exposure time, λ is the wavelength of the incident light, and F is the f-number of the optical system.

Therefore the final expression for intensity distribution for a single bar in the presence of motion becomes

$$i(V) = 2(\pi)^{-1} \int_0^2 D(\omega) \frac{\sqrt{I_1^2 + I_2^2}}{2\sqrt{\omega A}} \cos (V\omega - \theta')$$
$$\cdot \sin (\omega L) (\omega^{-1})d\omega \qquad (8)$$

The object spectrum for a triangular-

shaped object[30] and an object in the shape of a single cycle of a sinusoid are given respectively by

$$O(\omega) = (\pi\omega^2)^{-1} \sin^2(\omega L) \qquad (9)$$

and

$$O(\omega) = \left[2\omega\left(\pi^2 - 4\omega^2 L^2\right)\right]^{-1} \pi \sin(2\omega L) \quad (10)$$

By using these relations respective images can be calculated.

However, there is a complication in defining and computing the modulation of the image because any peak value against a background of 0.0 gives a modulation of 1.0 when calculated according to the conventional formula, namely,

Modulation $= (I_{max} - I_{min})/(I_{max} + I_{min})$

where I_{max} is the peak value and I_{min} is the background. Williams[4] has shown that the final modulation of a single bar target of original modulation Mo, which is degraded according to some MTF, is equl to $b \times Mi$ where b is the final peak value in normalised intensity units of an equal size bar image with an input intensity and modulation of 1.0, which has been degraded by the same MTF. Therefore, the final modulation of bar images which had an input intensity and modulation 1.0 is defined to be their maximum intensity or effective exposure value b. Considering this definition as an extension from the cases where the input modulation is less than 1.0, this definition is very clear. It must be noted that this definition may be extended to define a logarithmic contrast as was done by Charman[5]. However, we characterize our images by the ordinary contrast, i.e., the modulation.

RESULTS AND DISCUSSIONS

Intensity distributions were calculated numerically on an electronic computer using 32-point Gauss Quadrature method for $2L = 2.0, 4.0, 8.0, 12.0,$ and 16.0. Some representative results of calculations are shown graphically in Figures 1 through 4 for bar widths $2L = 2.0$ and 8.0 diffraction units. The results in the absence of image motion ($A = 0.0$) are also shown for the sake of comparison by the dotted curves in Figures 1, 3, and 4. Figure 1 demonstrates the influence of parabolic image motion on the bar images formed by annular aperture systems with an obstruction ratio $\eta = 0.25, 0.50,$ and 0.75.

In all the three cases, it is observed that the secondary maxima in the motion-free images arising due to diffraction at the annular aperture are no longer visible in the
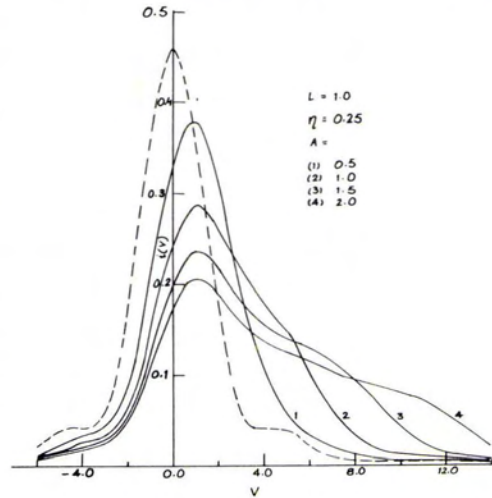

Fig. 1. (a) Images of bar in the presence of parabolic motion for L = 1.0, η = 0.25 for A = 0.0, 0.5, 1.0, 1.5, and 2.0.
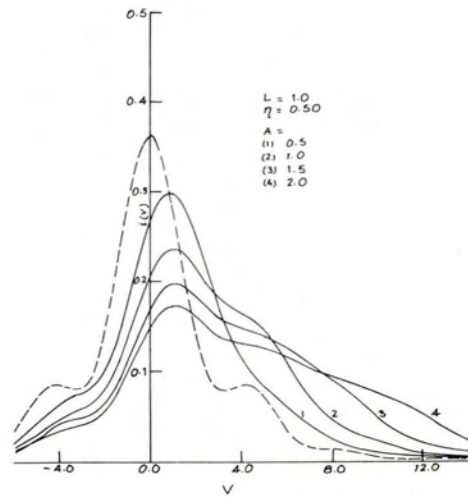

Fig. 1 (b) Same as 1(a) for η = 0.50.

motion-degraded images and degradation becomes more deleterious for higher values of η; also, there is broadening of the diffraction figure with increasing value of η and A. It must therefore be stressed that increasing obscuration leads to more stringent tolerance on the acceptable level of motion. This is because the contrast in the images of extended objects formed by systems with pupil obscuration is reduced cumulatively by the obscuration and the image motion. Clearly, more efficient image-motion compensation/stabilization techniques must be developed for annular aperture systems than are availa-
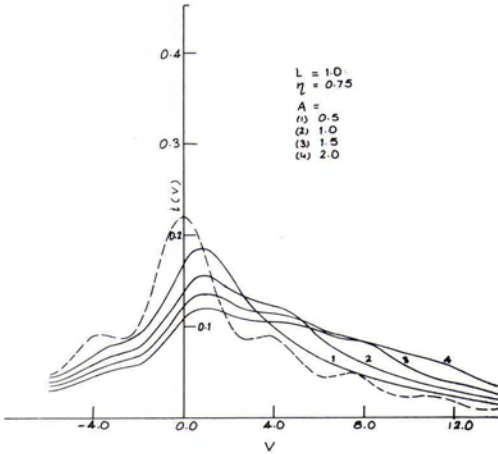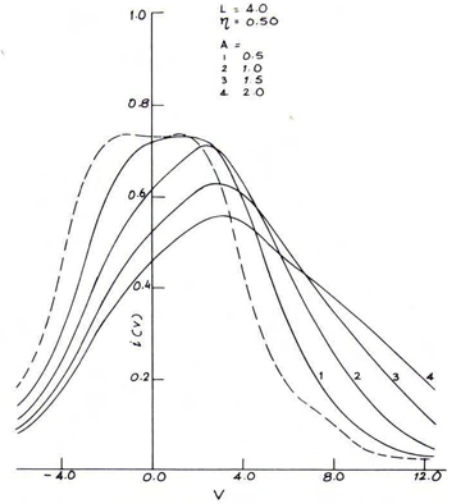
FIG. 1 (c)   Same as 1(a) for $\eta = 0.75$.

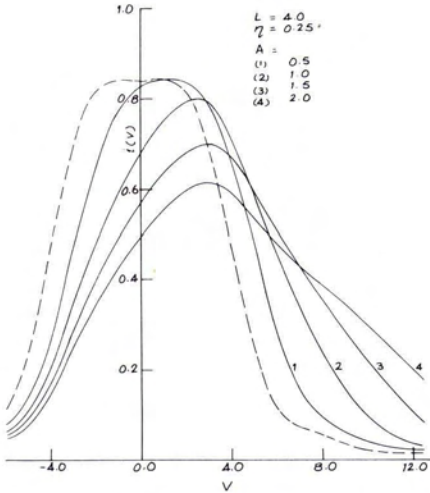

FIG. 1 (e)   Same as 1(a) for L = 4.0 and $\eta = 0.50$.

FIG. 1 (d)   Same as 1(a) for L = 4.0 and $\eta = 0.25$.

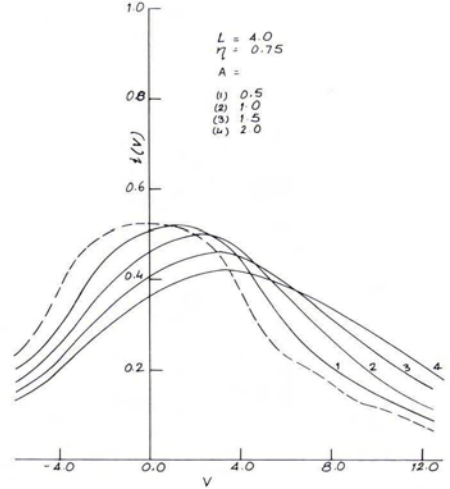

FIG. 1 (f)   Same as 1(a) for L = 4.0 and $\eta = 0.75$.

ble for conventional circular aperture systems.

It is interesting to note from Figure 1 that a shift in the position of peak intensity is observed in going from $A = 0.0$ to 0.50 but it remains constant for higher values of A. This is explained on the basis of the fact that the phase part of the transfer function of parabolic motion becomes oscillatory beyond a certain value of ω for given value of A (for example at $\omega = 0.7$, for $A = 1.0$) and then becomes constant afterwards in the high frequency region. Intensity distribution is asymmetric with respect to origin in the presence of motion because θ' is a nonlinear function of ω. Such asymmetry is also ob-

served in investigating the comatic images by Ingelstam et al.[31] and Barakat[32].

Figure 1 also shows that the central intensity increases as the width of the bar is increased for the same amount of motion. Intensity decreases with the increasing value of motion parameter for the same bar width. For large values of L the bar object behaves as disk or an edge object. Figure 2 shows the plots of the modulation of the final images as a function of the image-motion parameter for different values of L when the object is in the form of a single cycle of pure sinusoid, a triangle, and a bar. It can easily be seen that the contrast is greater for a bar target than for a sinusoidal or triangular targets of the same
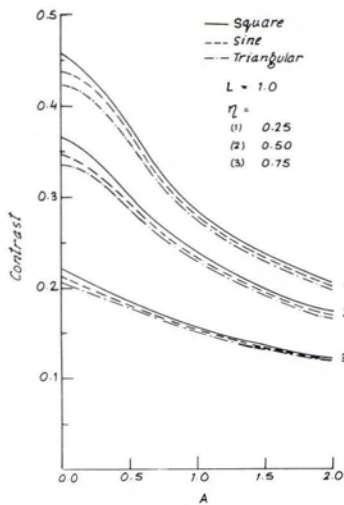
FIG. 2 (a)   Contrast in the images of bar, sinusoidal and triangular object with L = 1.0 for η = 0.25, 0.50 and 0.75.
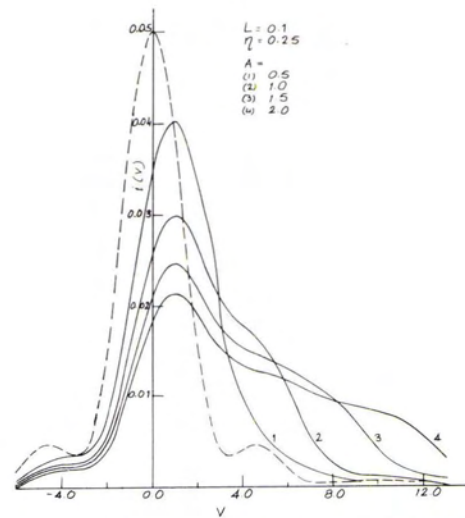

FIG. 3 (a)   Image of a line with L = 0.1, η = 0.25 for A = 0.0, 0.5, 1.0, 1.5, and 2.0.

FIG. 3 (b)   Same as 3(a) for η = 0.50.

period. This is due to the fact that square wave shape carries more energy than the narrow-peaked sine wave at the same period, and hence degrades less when both are blurred by convolution with the same spread function. However, the contrast becomes nearly the same for smaller values of L and η; therefore the difference in the images of these types of isolated extended but aperiodic objects are not considerable for low values of L and η. The difference is, however, appreciable for higher values.
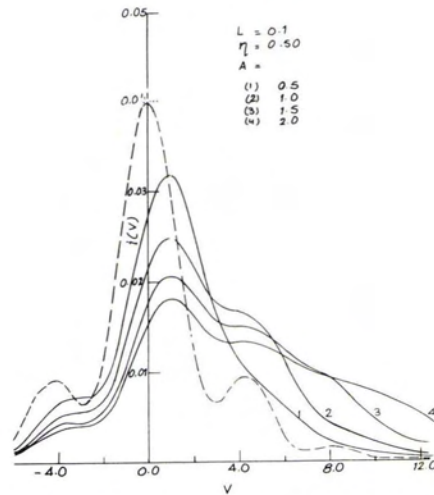
Figure 3 shows the plot of intensity distribution for very narrow bar (L = 0.1) and gives the line spread function for annular aperture system.

In Figure 4 contrast is plotted as a function of normalised frequency for various values of A and η. We find that the contrast never falls to zero for a bar of any finite width; however, it reduces with increasing values of η and A. The wide spectral bandwidth of a single bar provides an explanation for the frequent appearance in aerial photography of isolated objects.

CONCLUDING REMARKS

Rosenau,[24] while considering the perfor-
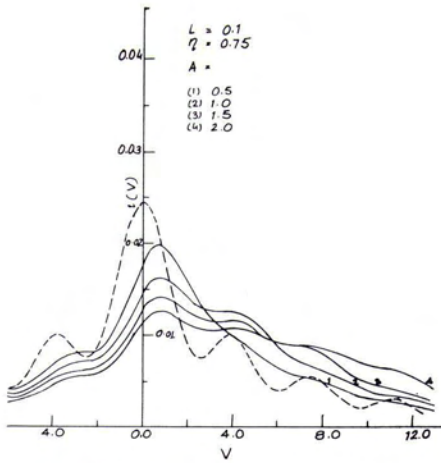

FIG. 2 (b)   Same as 2(a) for L = 4.0.
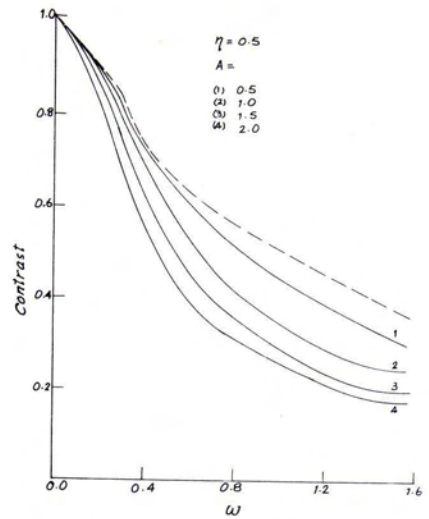
FIG. 3 (c)   Same as 3(a) for $\eta = 0.75$.
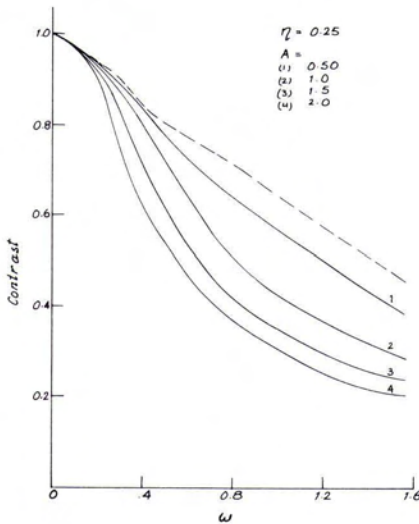

FIG. 4 (b)   Same as 4(a) for $\eta = 0.50$.

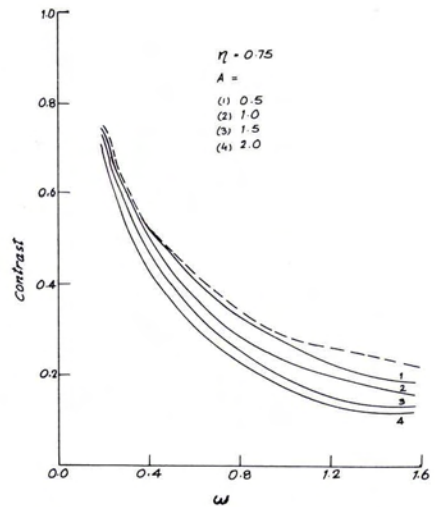FIG. 4 (a)   Single bar contrast transfer function for $\eta = 0.25$ for A = 0.0, 0.5, 1.0, 1.5, and 2.0.

FIG. 4 (c)   Same as 4(a) for $\eta = 0.75$.

mance of a model 501 light weight aerial panoramic camera, derived an expression for co-efficient B in the form

$$B = \tfrac{1}{2}\,(v/h)\,\dot{x}_f \sin \beta$$

where v is aircraft velocity relative to earth, h is altitude of film plane above the earth, $\dot{x}_f$ is the film velocity to compensate image motion, and β is scan angle. In a typical case, the camera was exposed for 1/55 sec at a maximum rate of 0.30 rad/sec with a film transport velocity of 10.4 in/sec. Thus, for a 60° scan angle, the total image movement during the time of exposure becomes

$$B \, te^2 = (1/88) \text{ mm}$$

Since in most of the photo—reconnaissance missions the sensor is kept at a very high altitude (as in a U-2 type aircraft or a satellite), a long focal lens having a large F-value is required[17]. Thus for $\lambda = 5000A°$ and $F = 5$ to 10 (say), the motion parameter

$$A = Bte^2/2\lambda F = 2.28 \text{ to } 1.14$$

This shows that the values of A considered in our computations are realistic.

It is now well known that the transfer

function of certain optical systems with appropriate amplitude filters is very similar to the transfer function of annular aperture systems[33]. Hence, the trends for motion-degraded bar spread function in these will be similar to our results. It may also be helpful in various applications using reflecting components such as in space optics[34], night vision aids[35], low-light-level systems[36], optical processing[17] of images, etc.

We would also like to mention that the motion-degraded images of two-dimensional objects such as disks, annuli, etc., cannot be calculated by using Equation 5 because the OTF of the total system does not possess a rotational symmetry but acquires a certain azimuthal dependence. Work in this context has been done by Rattan and Singh[37] and Gupta and Singh[38].

The problem of restoring images degraded by parabolic motion is under investigation and results will be reported at a later date.

REFERENCES

1. Brock, G. C., *Image Evaluation for Aerial Photography*, The Focal Press, London, 1970.
2. Lewis, N. W. and T. V. Hauser, "Micro Contrast and Blur in Imaging Systems", *J. Phot. Sci. 10* (1962) 288.
3. Stapleton, R. E., "The Sharpness of Photographic Materials", *J. Phot. Sci. 8* (1960) 14.
4. Williams, R., "A Re-examination of Resolution Prediction from Lens MTF's and Emulsion Thresholds", *Phot. Sci. Eng. 13* (1969) 252.
5. Charman, W. N., "Resolving Power and the Detection of Linear Detail", *Canadian Surveyor 29* (1965) 309.
6. Sokolo'sky, M. N., "Calculating the Image Contrast of a Point or Line Objects", *Sov. J. Opt. Tech. 40* (1973) 394.
7. Singh, K. and H. S. Dhillon, "Diffraction of partially Coherent Light by an Aberration Free Annular Aperture", *J. Opt. Soc. Am. 59* (1969) 395.
8. Singh, K. and A. K. Kavathekar, "Images of a General Periodic Bar Pattern Through an Aberration Free Annular Aperture", *J. Opt. Soc. Am. 59* (1969) 936.
9. Powell, I., "The Computation of Aberrational Diffraction Images for Catadioptric Systems", *Opt. Acta. 20* (1973) 879.
10. Powell, I., "The Calculation of the OTF for Systems with Central Obscurations, *Opt. Acta 21* (1974) 453.
11. Price, M. J. and B. Vinter, "Effect of Liquid Distortion and Aperture Shape on the Quality of Bubble Chamber Photographs", *Appl. Opt. 12* (1973) 271.
12. Tschunko, H. F. A., "Annular Aperture with Central Obstruction", *Appl. Opt. 13* (1974) 22.
13. Mangus, J. P. and J. H. Underwood, "Optical Design of a Glancing Incidence X-ray Telescope", *Appl. Opt. 8* (1969) 45.
14. Foreman Jr. J. W., G. H. Hunt, and E. K. Lawson, "Images of Truncated One Dimensional Periodic Bar Targets in Aberration Limited Optical Systems", *Appl. Opt. 10* (1971) 105.
15. McCrickerd, J. T., "Coherent Processing and Depth of Focus of Annular Aperture Imagery", *Appl. Opt. 10* (1971) 2226.
16. Nagel, M. R., ed., *Evaluation of Motion Degraded Images*, Proc. of a Seminar held in Cambridge, Mass. Dec. 3-5, 1968 (NASA, Washington, D.C. 1969).
17. Jensen, N., *Optical and Photographic Reconnaissance Systems*, John Wiley and Sons, New York, 1968.
18. Dubovik, A. S., *Photographic Recording of High Speed Process*, (Pergamon Press, Oxford, 1968).
19. Kowaliski, P., *Applied Photographic Theory*, John Wiley and Sons, N. Y. 1972.
20. Fouche, C., in *Space Optics*, eds; A. Maréchal and G. Courtes, Gordon and Breach Science Publ. N. Y., 1974, p. 379.
21. Singh, K. and N. K. Jain, "Images of Truncated Triangular Wave Periodic Targets in Optical Systems in the Presence of Linear Image Motion", *Nouv. Rev. Opt. 3* (1972) 309.
22. Singh, K., R. Rattan, and N. K. Jain, "Diffraction Images of Truncated Sine and Square Wave Periodic Objects in the Presence of Linear Image Motion", *Appl. Opt. 12* (1973) 1846.
23. Singh, K., R. Rattan, and J. N. Maggo, "Influence of Longitudinal Vibration on the Diffraction Images of Bright Incoherent Disks", *Appl. Opt. 14* (1975) 500.
24. Rosenau, M. D., "Parabolic Image Motion", *Photogram. Eng. 27* (1961) 421.
25. Som, S. C., "Analysis of Effect of Linear Smear on Photographic Images", *J. Opt. Soc. Am. 61* (1971) 859.
26. Rattan, R. and K. Singh, "Diffraction Images of one Dimensional Periodic Objects in the Presence of Quadratic Image Motion", *Atti. Fond. G. Ronchi. 27* (1972) 727.
27. Gupta, P. C. and K. Singh, "Application of Holographic Addition and Substraction to Quadratic Image Motion Analysis", *Pramana 3* (1974) 390.
28. Jablonwski, D. P. and S. H. Lee, "Restoration of Degraded Images by Composite Gratings in Coherent Optical Processor", *Appl. Opt. 12* (1973) 1703.
29. Sawchuk, A. A., "Space Variant Image Motion

Degradation and Restoration", *Proc. IEEE 60* (1972) 854.

30. Barakat, R. and A. Houston, "Diffraction Images of Single Bar in the Presence of Off-Axis Aberrations", *J. Opt. Soc. Am. 46* (1966) 1402 L.

31. Ingelstam, E., E. Djurle, and B. Sjögren, "Contrast Transmission Functions Determined Experimentally for Asymmetrical Images and For the Combination of Lens and Photographic Emulsions", *J. Opt. Soc. Am. 46* (1956) 707.

32. Barakat, R. and A. Houston, "Transfer Function of an Optical System in the Presence of Off-Axis Aberrations", *J. Opt. Soc. Am. 55* (1965) 1142.

33. Katti, P. K., K. Singh, and K. N. Chopra, "Effect of Non Uniform Aperture Illumination on the Rectangular Wave response of a Diffrac-

tion Limited Imaging System with a Slit Aperture", *Opt. Acta. 17* (1970) 299.

34. Cameron, R. M., M. Bader, and P. E. Mobley, "Design and Operation of the NASA 91.5 cm Airborne Telescope", *Appl. Opt. 10* (1971) 2011.

35. Amon, M., "Large Objective for Night Observation", *Appl. Opt. 10* (1971) 490.

36. Becker, J., "Optical Systems for Use at Low Light Levels", *Opt. Acta. 17* (1970) 481.

37. Rattan, R. and K. Singh, "Diffraction Images of Bright Incoherent Disks in the Presence of Transverse Sinusoidal Vibrations", *Nouv. Rev. Opt. 7* (1976). In Press.

38. Gupta, P. C. and K. Singh, "Image Quality in an Optical System Operating in Partially Coherent Light; Effect of Parabolic Motion", *Appl. Opt. 15* (1976). In Press.